Chapter 4

Comparative Study of Two-Dimensional Wavelets Scheme for Linear and Nonlinear Volterra Weakly Singular Partial Integro-Differential Equation Based on Operational Matrices

4.1 Introduction

In wide areas of physics and engineering systems which are function of space and time are generally described by differential equations. In some situations such a formulation may not purely model the physical system because while expressing the system as a function at a time, it fails to explanation and effect of past history. Therefore, there is arises a new type of equation, called integro-differential equations. The term integro-differential equations is applied to those equations in which the unknown functions appear with their derivatives and either the unknown functions or their derivatives or both, appear under the sign of integration. One of the first to study the integro-differential equations was Volterra. In 1913, he published lectures on integral and integro-differential equations. Later, in 1931, he provided a classification of integro-differential equations [133]. Integro-differential equations arise from many branches of science such as physical phenomena involving thermoelastic contact [134], theory of heat conduction ([135], [136]), Viscoelasticity [137], control theory, ecological and epidemiological systems ([138],[139] and finan-

cial mathematics and option pricing ([140], [141], [142], [143]). Numerical solution of IDEs is considered by many authors. However the most papers are devoted to the ordinary IDEs, see for example ([144], [145], [146], [147], [148], [144], [149], [150], [151], [152], [153], [154]).

Partial integro-differential equations also have been studied in some papers. Finite difference scheme is proposed for weakly singular PIDEs in [170]. Finite element methods are developed in [155] to solve nonlinear parabolic and hyperbolic PIDEs with smooth kernels. An explicit integration method for solving a parabolic PIDE is presented in [156]. Semidiscrete finite element method is considered in ([157], [158], [173], [159]) for parabolic IDEs. Finite difference methods combined with the domain truncation technique using fully transparent artificial boundary conditions are proposed in [161] for numerical solution of parabolic Volterra IDEs on unbounded spatial domains. Spectral collocation method is proposed and analyzed in [162] for PIDEs with weakly singular kernel. An analysis of hyperbolic PIDEs is discussed in [160] by spectral method. Finite volume method is developed in [163] for solving elliptic PIDEs. Numerical solution of fourth order PIDEs is considered by quintic B-spline in [165] and Crank-Nicolson/quasi-wavelets in [164]. Also quasi-wavelet based numerical method for a class of PIDEs is presented in [167]. Discontinuous Galerkin method is developed in [166] for parabolic IDEs. An explicit/implicit Galerkin domain decomposition is discussed in [168] for parabolic IDEs.In the twentieth century decade, many considerable works on theoretical analysis ([169],[170],[171], [172], ([173],[174],[175]) have been carried on. Xu ([174], [175] considered backward Euler method in time direction for a parabolic integro-differential equation and derived the stability and convergence properties of the time discretizations. Lopez-Marcos [176] studied the nonlinear partial integro-differential equation. Yan and Fairweather [169] presented orthogonal spline collocation method for some partial integro-differential equations with smooth integral kernels. Approximate solution of the nonlinear Volterra PIDE in (4.1) is proposed in [177] based on the Legendre basis function with operational matrices.

A two-dimensional Volterra PIDEs solution have been addressed using two-dimensional Legendre and Chebyshev wavelet with associate its operational matrices. In present chapter, we concentrated on Volterra PIDE in bounded domain ($[0,1] \times [0,1]) = \Omega \subseteq \mathbf{R}^2$) as follows (see [177]):

$$u_y = u(x,y) + f(x,y) + \int_0^x \int_0^y \frac{Bu(s,t)}{(x-s)^\alpha} dtds \qquad 0 \leq x \leq 1,\ 0 \leq y \leq 1, \qquad (4.1)$$

subject to the initial condition

$$u(x,0) = u_0(x), \qquad 0 \leq x \leq 1.$$

Where B is *linear* or *nonlinear* differential operator, $0 < \alpha < 1$, $(x,y) \in \Omega$, $f(x,y)$, $u_0(x)$ are known functions, and u is the real unknown function in Ω is sought for $0 \leq x \leq 1,\ 0 \leq y \leq 1$, which will be determined in the present paper. It can be seen that in *Eq.*(4.1) the kernel function has a singularity at $s = x$. The function $f(x,y)$ and $u(x,y)$ are assumed to be sufficiently smooth in order to assure the existence and uniqueness of a solution $u \in C(\Omega)$. *Eq.*(4.1) affords a simple model equation that combines the derivative with a *weak singularity.* Analytic solution of *Eq.*(4.1) is not an easy task , so it required to provide some accurate numerical schemes for solving such problems. A convenient way to treating such problems is to reduce them to algebraic equations via operational matrices. This can be done in several ways; we will discuss one approach which is applicable in many cases and leads to efficient numerical procedures.

In this chapter, we constructed operational matrices for the Eq.(4.1), based on two dimension Legendre and Chebyshev wavelets approximations using Kronecker multiplications technique. It is well known that the operational matrix methods are very powerful tools for solving kinds of differential and weakly singular kernel with *nonlinear* integral equations specially with smooth function (see for instant ([177] and [178]). Throughout this chapter, we assume that initial condition u_0 in *Eq.*(4.1) is such that the *Eq.*(4.1) has a unique solution in Ω. We also assume

$u_x,\ u_{xx},\ u_y, u_{xy},\ u_{yy}$ are continuous for $0 \leq x \leq 1$ and $0 \leq y \leq 1$.

Wavelet analysis has been applied in a wide range of engineering discipline. For instance, they are implemented successfully in signal analysis time frequency analysis and fast algorithms for easy implementation (see[179], [180], [28], [181]and [182]). The application of wavelets for computing the numerical solutions of PDEs has been recently studied in both of the theoretical and computational points of view in a huge size of research works ([183], [184], [185], [186], [187], [188], [189], [190], [191]), in whch several efficient features of wavelets have been described, analysed and applied for solving PDEs. To solve a Volterra PIDEs numerically, we first need to find a finite dimensional approximation space for the solutions then discretize the Volterra PIDEs to a system of algebraic equations in that space, so that the numerical solution can be obtained. Recently, Singh et. al. ([177]), used polynomial approximation to find the numerical solution of the $Eq.(4.1)$. In this chapter, we have used wavelets approximation to find the numerical solution of the $Eq.(4.1)$. In many cases wavelets provide better basis (see for instance [192], [193], [194], [195]). The numerical wavelets operational matrix method presented in this chapter is based on reducing the equation to a system of algebraic equations by expanding the solution as two-dimensional Legendre and Chebyshev wavelets approximations with unknown coefficient. The characteristic of the operational matrix method is to transform the PIDEs into the algebraic system.

4.2 Function approximation

Suppose that $f(x, y)$ is an arbitrary function in $L^2(\Omega)$, then it can be approximated as follows:

$$F(x,y) = \sum_{n=1}^{2^{k-1}} \sum_{m=0}^{\infty} \sum_{n'=1}^{2^{k'-1}} \sum_{m'=0}^{\infty} F_{nmn'm'} \Phi_{nmn'm'}(x,y). \tag{4.2}$$

If the infinite series (4.2) is truncated for $m = M-1, m' = M'-1$, then approximation of *Eq.*(4.2) can be represented in the following form

$$F(x,y) \approx \sum_{n=1}^{2^{k-1}} \sum_{m=0}^{M-1} \sum_{n'=1}^{2^{k'}-1} \sum_{m'=0}^{M'-1} C_{nmn'm'} \Phi_{nmn'm'}(x,y) = F^T \Phi(x,y). \tag{4.3}$$

Where, F and Φ are $2^{k-1}2^{k'-1}MM' \times 1$, vector given as follows:

$$\begin{aligned} F = [&C_{1,0,1,0}, \cdots, C_{1,0,1,M'-1}, C_{1,0,2,0} \cdots, C_{1,0,2,M'-1}, \cdots, C_{1,0,2^{k'-1},0}, \cdots, \\ &C_{1,0,2^{k'-1},M'-1}, \cdots, C_{1,M-1,1,0}, \cdots, C_{1,M-1,1,M'-1}, C_{1,M-1,2,0}, \cdots, C_{1,M-1,2,M'-1}, \\ &C_{1,M-1,2^{k'-1},0} \cdots, C_{1,M-1,2^{k'-1},M'-1}, C_{2,0,1,0}, \cdots, C_{2,0,1,M'-1}, C_{2,0,2,0}, \cdots, \\ &C_{2,0,2,M'-1}, \cdots, C_{2,0,2^{k'-1},0}, \cdots, C_{2,0,2^{k'-1},M'-1}, \cdots, C_{2,M-1,1,0}, \cdots, C_{2,M-1,1,M'-1}, \\ &C_{2,M-1,2,0}, \cdots, C_{2,M-1,2,M'-1}, C_{2,M-1,2^{k'-1},0} \cdots, C_{2,M-1,2^{k'-1},M'-1}, \cdots, \\ &C_{2^{k-1},0,1,0}, \cdots, C_{2^{k-1},0,1,M'-1}, C_{2^{k-1},0,2,0}, \cdots, C_{2^{k-1},M-1,2^{k'-1},M'-1}]^T. \end{aligned} \tag{4.4}$$

And

$$\begin{aligned} \Phi = [&\Phi_{1,0,1,0}, \cdots, \Phi_{1,0,1,M'-1}, \Phi_{1,0,2,0} \cdots, \Phi_{1,0,2,M'-1}, \cdots, \Phi_{1,0,2^{k'-1},0}, \cdots, \\ &\Phi_{1,0,2^{k'-1},M'-1}, \cdots, \Phi_{1,M-1,1,0}, \cdots, \Phi_{1,M-1,1,M'-1}, \Phi_{1,M-1,2,0}, \cdots, \Phi_{1,M-1,2,M'-1} \\ &\Phi_{1,M-1,2^{k'-1},0} \cdots, \Phi_{1,M-1,2^{k'-1},M'-1}, \Phi_{2,0,1,0}, \cdots, \Phi_{2,0,1,M'-1}, \Phi_{2,0,2,0} \cdots, \\ &\Phi_{2,0,2,M'-1}, \cdots, \Phi_{2,0,2^{k'-1},0}, \cdots, \Phi_{2,0,2^{k'-1},M'-1}, \cdots, \Phi_{2,M-1,1,0}, \cdots, \Phi_{2,M-1,1,M'-1}, \\ &\Phi_{2,M-1,2,0}, \cdots, \Phi_{2,M-1,2,M'-1} \Phi_{2,M-1,2^{k'-1},0} \cdots, \Phi_{2,M-1,2^{k'-1},M'-1}, \cdots, \Phi_{2^{k-1},0,1,0}, \cdots, \\ &\Phi_{2^{k-1},0,1,M'-1}, \cdots, \Phi_{2^{k-1},0,2^{k'-1},0}, \cdots, \Phi_{2^{k-1},0,2^{k'-1},0}, \cdots, \Phi_{2^{k-1},M-1,2^{k'-1},M'-1}]^T. \end{aligned} \tag{4.5}$$

Theorem 4.2.1 *The series solution* $f(t) = \sum_{n=1}^{\infty} \sum_{m=0}^{\infty} f_{nm} \Phi^L(t)$ *define in Eq.*(1.9) *using Legendre wavelet approximation converges to* $f(t)$.

Proof See [197].

Theorem 4.2.2 *A function* $f(t)$ *defined on* $[0, 1)$ *with bounded second derivative* $|f''(t)| < B$, *can be expanded as an infinite sum of Chebyshev wavelet approximation defined in Eq.*(1.13) *and the series converges uniformly to the function* $f(t)$, *that is,*

$$f(t) = \sum_{n=1}^{\infty} \sum_{m=0}^{\infty} f_{nm} \Phi_{nm}^C(t).$$

Proof See [36].

Theorem 4.2.3 *The series solution* $f(x, y) = \sum_{n=1}^{2^{k-1}} \sum_{m=0}^{\infty} \sum_{n'=1}^{2^{k'-1}} \sum_{m'=0}^{\infty} c_{nmn'm'} \Phi(x, y)$ *using two dimensional Legendre wavelet or Chebyshev wavelet approximations converges to* $f(x, y)$.

Proof Let $L^2(\Omega)$ be the Hilbert space and $\Phi(x, y)$ be orthonormal wavelet basis (Legendre/Chebyshev) and for fixed k and k',

$$f(x, y) = \sum_{m=0}^{M-1} \sum_{m'=0}^{M'-1} c_{nmn'm'} \Phi(x_{nm}, y_{n'm'})$$

where $c_{nmn'm'} = \langle f(x, y), \Phi(x_{nm}, y_{n'm'} \rangle$.

Now, truncated above series upto N level, we get

$$f(x, y) = \sum_{m=0}^{N} \sum_{m'=0}^{N} c_{nmn'm'} \Phi(x_{nm}, y_{n'm'})$$

Let us denote $\Phi(x_{nm}, y_{n'm'}) = \Phi(x, y)$ and $\alpha_{ij} = \langle f(x, y), \Phi(x_i, y_j) \rangle$

Now,we define a sequence of partial sum S_N of $(\alpha_{ij} \Phi(x_i, y_j))$. Let S_N and S_M be the partial sums with $N \geq M$. We have to prove S_N is a Cauchy sequence in Hilbert space.

Let $S_N = \sum_{i=1}^{N} \sum_{j=1}^{N} \alpha_{ij} \Phi(x_i, y_j)$.

Now,

$$\langle f(x,y), S_N\rangle = \langle f(x,y), \sum_{i=1}^{N}\sum_{j=1}^{N}\alpha_{ij}\Phi(x_i,y_j)\rangle$$

$$= \sum_{i=1}^{N}\sum_{j=1}^{N}\overline{\alpha_{ij}}\langle f(x,y), \Phi(x_i,y_j)\rangle$$

$$= \sum_{i=1}^{N}\sum_{j=1}^{N}\overline{\alpha_{ij}}\alpha_{ij}$$

$$= \sum_{i=1}^{N}\sum_{j=1}^{N}|\alpha_{ij}|^2.$$

Now, we claim that

$$\|S_N - S_M\| = \sum_{i=M+1}^{N}\sum_{j=M+1}^{N}|\alpha_{ij}|^2, \quad for \quad N \geq M.$$

Since

$$\|S_N - S_M\|^2 = \|\sum_{i=1}^{N}\sum_{j=1}^{N}\alpha_{ij}\Phi(x_i,y_j) - \sum_{k=1}^{M}\sum_{l=1}^{M}\alpha_{lk}\Phi(x_k,y_l)\|^2$$

$$= \|\sum_{i=M+1}^{N}\sum_{j=M+1}^{N}\alpha_{ij}\Phi(x_i,y_j)\|$$

$$= \langle \sum_{i=M+1}^{N}\sum_{j=M+1}^{N}\alpha_{ij}\Phi(x_i,y_j), \sum_{k=M+1}^{N}\sum_{l=M+1}^{N}\alpha_{lk}\Phi(x_l,y_k)\rangle$$

$$= \sum_{i=M+1}^{N}\sum_{j=M+1}^{N}\sum_{k=M+1}^{N}\sum_{l=M+1}^{N}\alpha_{ij}\overline{\alpha_{lk}}\langle\Phi(x_i,y_j), \Phi(x_l,y_k)\rangle$$

$$= \sum_{i=M+1}^{N}\sum_{j=M+1}^{N}|\alpha_{ij}|^2, \quad for \quad N \geq M.$$

From Bessel's inequality, we have

$$\sum_{i=M+1}^{N}\sum_{j=M+1}^{N}|\alpha_{ij}|^2$$

is convergent and hence

$$\|S_N - S_M\| \to 0 \quad as \quad N, M \to \infty.$$

So $\langle S_N \rangle$ is a Cauchy sequence in $L^2(\Omega)$, hence,

$$S_N \to s \quad (say).$$

Now,

$$\begin{aligned}
\langle s - f(x,y), \Phi(x_i, y_j)\rangle &= \langle s, \Phi(x_i, y_j)\rangle - \langle f(x,y), \Phi(x_i, y_j)\rangle \\
&= \langle \lim_{N\to\infty} S_N, \Phi(x_i, y_j)\rangle - \langle f(x,y), \Phi(x_i, y_j)\rangle \\
&= \lim_{N\to\infty} \langle S_N, \Phi(x_i, y_j)\rangle - \alpha_{ij} \\
&= \lim_{N\to\infty} \langle \sum_{i=1}^{N}\sum_{j=1}^{N} \alpha_{ij}\Phi(x_i, y_j), \Phi(x_k, y_l)\rangle - \alpha_{ij} \\
&= \lim_{N\to\infty} \alpha_{ij}\langle \Phi(x_i, y_j), \Phi(x_k, y_l)\rangle - \alpha_{ij} \\
&= \alpha_{ij} - \alpha_{ij} \\
&= 0.
\end{aligned}$$

Hence

$$f(x,y) = s.$$

Thus, $\sum_{i=1}^{N}\sum_{j=1}^{N} \alpha_{ij}\Phi(x_i, y_j)$ converge to f(x,y) as $N \to \infty$ and proved.

Remark 8 *By above theorem, we conclude that*

$$\|f(x,y) - f_N(x,y)\| \to 0, \quad as \quad N \to \infty.$$

4.3 Operational matrices

4.3.1 Operational matrix of integration for Legendre wavelet

Let $\Phi^L(x,y)$ be two dimensional Legendre wavelets defined in (1.9), then we have

$$\begin{aligned}\int_0^y \Phi^L(x,t)dt &= \int_0^y (\Phi^L(x)\otimes\Phi^L(t))dt\\ &= \Phi^L(x)\otimes(\int_0^y \Phi^L(t)dt)\\ &\approx (I\Phi^L(x))\otimes(P\Phi^L(y))\\ &= (I\otimes P)(\Phi^L(x)\otimes\Phi^L(y))\\ &= P_y^L\Phi^L(x,y),\end{aligned}$$

so,

$$\int_0^y \Phi^L(x,t)dt \approx P_y^L\Phi^L(x,y), \tag{4.6}$$

where, I is $2^{k-1}M\times 2^{k-1}M$ identity matrix and $P_y^L = I\otimes P$ is a $2^{k-1}2^{k'-1}MM'\times 2^{k-1}2^{k'-1}MM'$ matrix (see [197]). Similarly,

$$\int_0^x \Phi^L(s,y)ds \approx P_x^L\Phi^L(x,y), \tag{4.7}$$

where, I is $2^{k-1}M\times 2^{k-1}M$ matrix and $P_x = P\otimes I$ is a $2^{k-1}2^{k'-1}MM'\times 2^{k-1}2^{k'-1}MM'$ matrix (see [197]).

4.3.2 Operational Matrix for integration for Chebyshev wavelet

Let $\Phi^c(x,y)$ be two dimensional Chebyshev wavelets defined in (1.13), then

$$\begin{aligned}\int_0^x \Phi^c(s,y)ds &= \int_0^x (\Phi^c(s)\otimes\Phi^c(y))ds\\ &= (\int_0^x \Phi^c(s)ds)\otimes\Phi^c(y)\\ &\approx (Q\Phi^c(x))\otimes(I\Phi^c(y))\\ &= (Q\otimes I)(\Phi^c(x)\otimes\Phi^c(y))\\ &= P_x^c\Phi^c(x,y),\end{aligned}$$

so,

$$\int_0^x \Phi^c(s,y)ds \approx P_x^c\Phi(x,y) \tag{4.8}$$

where, I is $2^{k-1}M\times 2^{k-1}M$ matrix and $P_x^c = P\otimes I$ is a $2^{k-1}2^{k'-1}MM'\times 2^{k-1}2^{k'-1}MM'$ matrix (see [196]).

Similarly,

$$\int_0^y \Phi(s,y)ds \approx P_y^c\Phi(x,y) \tag{4.9}$$

where, I is $2^{k-1}M\times 2^{k-1}M$ matrix and $P_y^c = P\otimes I$ is a $2^{k-1}2^{k'-1}MM'\times 2^{k-1}2^{k'-1}MM'$ matrix (see [196]).

4.3.3 Legendre wavelet operational matrix of differentiation

Let $\Phi^L(t,x)$ be two-dimensional Legendre wavelets defined in (1.9) then derivatve matrix as follows:

$$\begin{aligned}\frac{\partial}{\partial x}\Phi^L(x,y) &= \frac{\partial}{\partial x}(\Phi^L(x)\otimes\Phi^L(y))\\ &= (D^L\Phi^L(x))\otimes(I\Phi^L(y))\end{aligned}$$

$$= (D^L \otimes I)(\Phi^L(x) \otimes \Phi^L(y))$$

$$= D_x^L \Phi^L(x, y),$$

so,

$$\frac{\partial}{\partial t}\Phi^L(x, y) = D_x^L \Phi^L(x, y), \tag{4.10}$$

where, $D_x^L = D^L \otimes I$ is the matrix of order $2^{k-1}2^{k'-1}MM'$ (see [195]) and also I is the identity matrix. Similarly,

$$\frac{\partial}{\partial y}\Phi^L(x, y) = D_y^L \Phi^L(x, y), \tag{4.11}$$

where, $D_y^L = I \otimes D^L$ is a $2^{k-1}2^{k'-1}MM' \times 2^{k-1}2^{k'-1}MM'$ matrix (see [195]) and also I is the identity matrix.

4.3.4 Chebyshev wavelet operational matrix of differentiation

Let $\Phi^c(x, y)$ be two-dimensional Chebyshev wavelets defined in $Eq.(1.13)$ then derivative matrix as follows:

$$\frac{\partial}{\partial x}\Phi^c(x, y) = \frac{\partial}{\partial t}(\Phi^c(x) \otimes \Phi^c(y))$$

$$= (D^c \Phi^c(x)) \otimes (I\Phi^c(y))$$

$$= (D^c \otimes I)(\Phi^c(x) \otimes \Phi^c(y))$$

$$= D_x^c \Phi^c(x, y),$$

so,

$$\frac{\partial}{\partial x}\Phi^c(x, y) = D_x^c \Phi^c(x, y), \tag{4.12}$$

where, $D_x^c = D^c \otimes I$ is the matrix of order $2^{k-1}2^{k'-1}MM'$ (see [80]) and also I is the identity matrix. Similarly,

$$\frac{\partial}{\partial y}\Phi^c(x,y) = D_y^c \Phi^c(x,y), \tag{4.13}$$

where, $D_y^c = I \otimes D^c$ is a $2^{k-1}2^{k'-1}MM' \times 2^{k-1}2^{k'-1}MM'$ matrix (see [80]) and also I is the identity matrix.

4.3.5 Almost operational matrix of integration with singularity for variable x

Let $\Phi^c(x,y)$ be two dimensional wavelets(Legendre and Chebyshev) defined in (1.9) and (1.13) for $0 < \alpha < 1$ then,we get

$$\begin{aligned}
\int_0^x \frac{\Phi(a,y)}{(x-a)^\alpha} da &= \int_0^x \frac{\Phi(a) \otimes \Phi(y)}{(x-s)^\alpha} ds \\
&= \int_0^x \frac{\Phi(a)}{(x-a)^\alpha} da \otimes \Phi(y) \\
&\approx (V\Phi(x)) \otimes (I\Phi(y)) \\
&= (V \otimes I)(\Phi(x) \otimes \Phi(y)) \\
&= P_x^s \Phi(x,y),
\end{aligned}$$

so,

$$\int_0^x \frac{\Phi(a,y)}{(x-a)^\alpha} da \approx P_x^s \Phi(x,y), \tag{4.14}$$

where, $P_x^s = V \otimes I$, I is identity matrix and V defined in appendix subsections 6.2.1 and 6.2.2 for $M = 3$.

4.3.6 Product operational matrix

The following property of the product of two vectors $\Theta(x,y)$ and $\Theta^T(x,y)$ will also be used. Let

$$\Theta(x,y)\Theta^T(x,y)F \simeq \widetilde{F}\Theta(x,y). \tag{4.15}$$

Where, F is defined by (4.4) and $\widetilde{F}$ is $(N+1)^2 \times (N+1)^2$ product operational matrix (see [98]). Hence, using subsection (4.3.1), we get

$$\begin{aligned}
\int_0^x \int_0^y \frac{\Phi(a,b)}{(x-a)^\alpha} dadb &= \int_0^x \int_0^y \frac{\Phi(a) \otimes \Phi(b)}{(x-a)^\alpha} dadb \\
&= \int_0^x \frac{\Phi(a)}{(x-a)^\alpha} da \otimes \int_0^y \Phi(b) db \\
&\approx (P_x^s \Phi(x)) \otimes (P_y \Phi(y)) \\
&= (P_x^s \otimes P_y)(\Phi(x) \otimes \Phi(y)) \\
&= P_{xy}^s \Phi(x,y),
\end{aligned}$$

so,

$$\int_0^x \int_0^y \frac{\Phi(a,b)}{(x-a)^\alpha} dadb \approx P_{xy}^s \Phi(x,y),$$

where, $P_{xy}^s = P_x^s \otimes P_y$.

4.4 Numerical method of the solution

Representing the $Eq.(4.1)$ via expansion (see Table 4.1.):

Table 4.1: List of denotation

General symbol	**Uses of LWA**	**Uses of CWA**
$\Phi(t,x)$	$\Phi^L(t,x)$	$\Phi^c(t,x)$
P_y	P_y^L	P_y^c
P_x	P_x^L	P_x^c
P_{xy}^s	P_{xy}^L	P_{xy}^c
D_y	D_y^L	D_y^c
D_x	D_x^L	D_x^c
K_p	K_p^L	K_p^c

4.4.1 Type I-Numerical solution for linear PIDEs

Let us consider the weakly singular PIDEs $Eq.(4.1)$ for $Bu(x,y) = u_{yy}(x,y)$ as following:

$$\frac{\partial u(x,y)}{\partial y} = u(x,y) + f(x,y) + \int_0^x \int_0^y \frac{u_{tt}(s,t)}{(x-s)^\alpha} dsdt \quad 0 \le s \le x,\ 0 \le t \le y, \tag{4.16}$$

with initial condition $u(x,0) = u_0(x)$.

To find the solution of above problem, we will start with the approximations of

$u_y(x,y)$, $f(x,y)$ and $u_0(x)$ as follows

$$u_y(x,y) \approx C^T \Phi(x,y), \tag{4.17}$$

where, C^T is unknown.

Also,

$$f(x,y) \approx F^T \Phi(x,y), \tag{4.18}$$

$$u_0(x) \approx U^T \Phi(x,y). \tag{4.19}$$

Integrating $Eq.(4.17)$ w. r. t. y, we get

$$u(x,y) = u_0(x) + C^T \int_0^y \Phi(x,s)ds = U^T \Phi(x,y) + C^T \int_0^y \Phi(x,s)ds. \tag{4.20}$$

Using $Eqs.(4.19)$ and (4.20), We get

$$u(x,y) = U^T \Phi(x,y) + C^T P_y \Phi(x,y) = (U^T + C^T P_y)\Phi(x,y). \tag{4.21}$$

Differentiating $Eq.(4.21)$ two time w. r. t. y, we get

$$u_{yy}(x,y) = (U^T + C^T P_y)(D_y^T)^2 \Phi(x,y). \tag{4.22}$$

Now,

$$\int_0^x \int_0^y \frac{u_{tt}(s,t)}{(x-s)^\alpha} dtds = (U^T + C^T P_y)(D_y^T)^2 \int_0^x \int_0^y \frac{\Phi(s,t)}{(x-s)^\alpha} dsdt,$$

or,

$$\int_0^x \int_0^y \frac{u_{tt}(s,t)}{(x-s)^\alpha} dtds = (U^T + C^T P_y)(D_y)^2 P_{xy}^s \Phi(x,y). \tag{4.23}$$

Combining $Eq.(4.16)$ to $Eq.(4.23)$, we get

$$C^T\Phi(x,y) = (U^T + C^T P_y)\Phi(x,y) + F^T\Phi(x,y) + (U^T + C^T P_y)(D_y)^2 P^s_{xy})\Phi(x,y),$$

so by above equation, we get

$$C^T = (U^T + F^T + U^T(D_y)^2 P^s_{xy})(I - P_y - P_y(D_y)^2 P^s_{xy})^{-1}. \tag{4.24}$$

Substituting $Eq.(4.24)$ back into the $Eq.(4.21)$, we finally have the numerical solution as follows

$$u(x,y) = (U^T + F^T + U^T(D_y)^2 P^s_{xy})(I - P_y - P_y(D_y)^2 P^s_{xy})^{-1}\Phi(x,y). \tag{4.25}$$

Now, we use the collocation method for solving $Eq.(4.25)$. For this, we suppose $x = \{x_i\}_{i=1}^N = \frac{i}{N}$ and $y = \{y_j\}_{j=1}^N = \frac{j}{N}$ are the set of (N) nodes. We substitute these nodes in $Eq.(4.25)$ and hence $Eq.(4.16)$ solved numerically.
Similarly, we may find a method for PIDEs $Eq.(4.1)$ at $Bu(x,y) = u_{xx}(x,y)$ and $Bu(x,y) = u_{xy}(x,y)$ as in $Eq.(4.16)$ for $Bu(x,y) = u_{yy}(x,y)$.

4.4.2 Type II-Numerical solution for nonlinear PIDEs

For *type II* singular PIDEs we take $Bu = [u(x,y)]^p$ in $Eq.(4.1)$,where p is positive integer. Then we have from $Eq.(4.1)$

$$u_y = u(x,y) + f(x,y) + \int_0^x \int_0^y \frac{[u(\zeta,\eta)]^p}{(x-\zeta)^\alpha} d\eta d\zeta \tag{4.26}$$

along with the given conditions mention in $Eq.(4.1)$. To find the solution of problem $Eq.(4.26)$, we start with the approximations of u_y as follows

$$u_y \approx C^T\Phi(x,y), \tag{4.27}$$

where, C^T is unknown.

Integrating $Eq.(4.27)$ with respect to y, we get

$$u(x,y) = u_0(x) + C^T \int_0^y \Phi(x,s)ds = U^T\Phi(x,y) + C^T \int_0^y \Phi(x,s)ds,$$

or,

$$u(x,y) = U^T\Phi(x,y) + C^T P_y\Phi(x,y) = (U^T + C^T P_y)\Phi(x,y). \tag{4.28}$$

Put, $(U^T + C^T P_y) = E^T$ in $Eq.(4.28)$, then we have

$$u(x,t) = E^T\Phi(x,y). \tag{4.29}$$

Now, we calculate $[u(x,y)]^p$ by using the product operational matrix as

$$[u(x,y)]^2 \approx (E^T\Phi(x,y))(E^T\Phi(x,y)) = E^T\Phi(x,y)\Phi^T(x,y)E$$

$$= E^T\widetilde{E}\Phi(x,y) = E_2\Phi(x,y),$$

where, $E_2 = E^T\widetilde{E}$.

For $[\Phi(x,y)]^3$, we get

$$[u(x,y)]^3 \approx (E^T\Phi(x,y))(E_2\Phi(x,y)) = E^T\Phi(x,y)\Phi^T(x,y)E_2^T$$

$$= E^T\widetilde{E_2^T}\Phi(x,y) = E_3\Phi(x,y),$$

where, $E_3 = E^T\widetilde{E_2^T}$.

Similarly, we have

$$[u(x,y)]^p \approx E_p\Phi(x,y).$$

Combining $Eqs.(4.26)$, (4.27), (4.28),and (4.29) we get

$$C^T\Phi(x,y) = E^T\Phi(x,y) + F^T\Phi(x,y) + E_p\int_0^x\int_0^y \frac{\Phi(\zeta,\eta)}{(x-\zeta)^\alpha}d\eta d\zeta$$

or,

$$C^T\Phi(x,y) = E^T\Phi(x,y) + F^T\Phi(x,y) + E_pP^s_{xy}\Phi(x,y),$$

which implies that

$$C^T = E^T + F^T + E_pP^s_{xy}. \tag{4.30}$$

The above system of equation can be written as

$$f(C) = L(C) + N(C). \tag{4.31}$$

Where, $L(C) = C^T$ denotes the linear part and $N(C) = -(E^T + F^T + E_pP^s_{xy})$ denotes the non-linear part.

$Eq.(4.31)$ is a system of $2^{k-1}2^{k'-1}MM'$ non-linear equations in $2^{k-1}2^{k'-1}MM'$ unknowns, which can be solved for the elements of C^T by using the Newton-Raphson method. Then by putting the value of C^T into the $Eq.(4.28)$ we get $u(x,y)$ as an approximate solution of $Eq.(4.26)$.

4.4.3 Type III-Numerical solution for nonlinear PIDEs

For *type III* singular PIDEs we take $Bu = [\gamma_{i,j}u(x,y)]^p$ in $Eq.(4.1)$, $i,j = 0,1,2,\cdots,N$ with the condition that i,j can not be zero together, where, $\gamma_{i,j}\Phi(x,y)$ denotes the i times differentiation with respect to x and j times differentiation with respect to y of u. Then we have from $Eq.(4.1)$

$$u_y = u(x,y) + f(x,y) + \int_0^x\int_0^y \frac{[\gamma_{i,j}u(\zeta,\eta)]^p}{(x-\zeta)^\alpha}d\eta d\zeta, \tag{4.32}$$

To find the numerical solution of above equation, we approximate u_y as follows:

$$u_y \approx C^T \Phi(x, y) \tag{4.33}$$

where, C^T is unknown.

Also,

$$f(x, y) \approx F^T \Phi(x, y), \quad u_0(x) \approx U^T \Phi(x, y),$$

where, F^T and U^T are known.

Integrating $Eq.(4.33)$ with respect to y, then from $Eq.(4.29)$, we have

$$u(x, y) = E^T P_y \Phi(x, y). \tag{4.34}$$

Differentiating $Eq.(4.34)$, i times with respect to x and j times with respect to y,we get

$$\gamma_{i,j} u(x, y) = E^T P_y D_x^i D_y^j \Phi(x, y) = K\Phi(x, y), \; K = P_y D_x^i D_y^j$$

where, D_x is the operational matrix of differentiation of variable x and D_y is the operational matrix of differentiation of variable y. In order to calculate $[\gamma_{i,j} u(x, y)]^p$, we use the same approach as we did in the $type - I$ problem. So, we have

$$[\gamma_{i,j} u(x, y)]^p = K_p \Phi(x, y). \tag{4.35}$$

Using above approximations, $Eq.(4.32)$ reduces to

$$C^T \Phi(x, y) = E^T \Phi(x, y) + F^T \Phi(x, y) + K_p \widehat{S} \Phi(x, y).$$

Hence, we have

$$C^T = P_y^T + F^T + K_p \widehat{S}. \tag{4.36}$$

The above system of equation can be written as

$$f(C) = L(C) + N(C). \tag{4.37}$$

Where, $L(C) = C^T$ is the linear part and $N(C) = -(P_y + F^T + K_p\widehat{S})$ is the non-linear part.

$Eq.(4.37)$ is a system of $2^{k-1}2^{k'-1}MM'$ non-linear equations in $2^{k-1}2^{k'-1}MM'$ unknowns, which can be solved for the elements of C^T by using the Newton-Raphson method. Then by putting the value of C^T into the $Eq.(4.33)$ we get $u(x, y)$ as an approximate solution of $Eq.(4.32)$.

4.5 Convergence Analysis

4.5.1 For Legendre Wavelet

Theorem 4.5.1 *Let $(\frac{\partial u}{\partial y})_N(x, y)$ be the LWA of $(\frac{\partial u}{\partial y})(x, y)$ and assume that the mixed second derivative of $(\frac{\partial u}{\partial y})(x, y)$ is bounded by a constant $\Im$.i.e. $\left|\frac{\partial^4 u}{\partial x^2 \partial y^2}\right| < \Im$, then we have the following upper bound of error:*

$$\|u_y - (u_y)_N\|^2_{L^2} < \frac{\Im^2 \wp^2}{2^{18}},$$

where, $\wp$ is a polygamma function ,$\wp = F_3(-3/2 + N)$.

Proof See [198].

Lemma 4.5.2 *(Generalization of lemma (4.5.1)) Let $u(x, y)$ be the sufficiently smooth function in Ω and $(u_{yy})_N(x, y)$ be the LWA of $u_{yy}(x, y)$. Assume that the mixed second derivative of $u(x, y)$ is bounded by a constant ζ.*
i.e.$\left|\frac{\partial u^6(x,y)}{\partial x^2 \partial y^4}\right| < \zeta$, then ,we have the following upper bound of error :
$\| u_{yy} - (u_{yy})_N \| < \frac{\zeta\eta}{2^{18}}$, *where, $\eta = F_3(\frac{-3}{2} + N)^2$.*

Proof Proof is similar to the proof of *theorem*(4.5.1).

Lemma 4.5.3 *(Generalization of lemma* (4.5.1) *) Let* $u(x,y)$ *be the sufficiently smooth function in* Ω *and* $(u_{xx})_N(x,y)$ *be the LWA of* $u_{xx}(x,y)$*. Assume that the mixed second derivative of* $u(x,y)$ *is bounded by a constant* θ*.*
i.e.$\left|\frac{\partial u^6(x,y)}{\partial x^4 \partial y^2}\right| < \theta$*, then ,we have the following upper bound of error :*
$\| u_{xx} - (u_{xx})_N \| < \frac{\theta\eta}{2^{18}}$, *where,* $\eta = F_3(\frac{-3}{2} + N)^2$.

Proof Proof of lemma can be find using proof of *theorem*(4.5.1) and lemma (4.5.2).

4.5.2 For Chebyshev Wavelet

Theorem 4.5.4 *Let* $u(x,y)$ *be the sufficiently smooth function in* Ω *and* $\left(\frac{\partial^\Lambda u(x,y)}{\partial y^\Lambda}\right)_N$, $\Lambda \geq 0$*, be the Chebyshev wavelet approximation of* $\left(\frac{\partial^\Lambda u(x,y)}{\partial y^\Lambda}\right)$ *and assume that the mixed derivative of* $\left(\frac{\partial^\Lambda u(x,y)}{\partial y^\Lambda}\right)$ *is bounded by a constant* K_2*.i.e.*

$$\left|\frac{\partial^{\Lambda+2} u(x,y)}{\partial x \partial y^{\Lambda+1}}\right| < K_2,$$

then we have the following upper bound of error:

$$\left\| \left(\frac{\partial^\Lambda u(x,y)}{\partial y^\Lambda}\right) - \left(\frac{\partial^\Lambda u(x,y)}{\partial y^\Lambda}\right)_N \right\|^2_{L^2} < \frac{K_2^2}{2}(F[1,N])^2,$$

where $F[1,N]$ *is polygamma function.*

Proof See [198].

Remark 9 *It is comprehensible that at* $m = m' = 0$ $\{\Phi^c_{nmn'm'}\}$ *form an orthonormal system constructed by Haar scaling function with respect to the weight function and thus the series*

$$\sum_{n=1}^{2^{k-1}} \sum_{n'=1}^{2^{k'-1}} C_{n,0,n',0} \Phi_{n,0,n',0}(x,y)$$

is convergent. So,

$$\left|\sum_{n=1}^{2^{k-1}}\sum_{m=0}^{\infty}\sum_{n'=1}^{2^{k'-1}}\sum_{m'=0}^{\infty} C_{nmn'm'}\Phi_{nmn'm'}(x,y)\right| \leq \left|\sum_{n=1}^{2^{k-1}}\sum_{n'=1}^{2^{k'-1}} C_{n0n'0}\Phi_{n0n'0}(x,y)\right| + \left|\sum_{n=1}^{2^{k-1}}\sum_{m=1}^{\infty}\sum_{n'=1}^{2^{k'-1}}\sum_{m'=1}^{\infty} C_{nmn'm'}\Phi_{nmn'm'}(x,y)\right| < \infty.$$

Hence, $|C_{nmn'm'}|$ is absolutely convergent.

Lemma 4.5.5 *Let $u(x,y)$ be the sufficiently smooth function in Ω and $\left(\frac{\partial^2 u(x,y)}{\partial y^2}\right)_N$ be the CWA of $\left(\frac{\partial^2 u(x,y)}{\partial y^2}\right)$ and assume that the mixed derivative of $\left(\frac{\partial^2 u(x,y)}{\partial y^2}\right)$ is bounded by a constant K_2.i.e.*

$$\left|\frac{\partial^3 u(x,y)}{\partial x \partial y^2}\right| < S_1,$$

then we have the following upper bound of error:

$$\left\|\frac{\partial^2 u(x,y)}{\partial y^2} - \left(\frac{\partial^2 u(x,y)}{\partial y^2}\right)_N\right\|_{L^2}^2 < \frac{S_1^2}{2}(F[1,N])^2,$$

where, $F[1,N]$ is polygamma function.

Proof Proof is similar as *theorem* (4.5.4), if $\Lambda = 2$.

Lemma 4.5.6 *Let $u(x,y)$ be the sufficiently smooth function in Ω and $\left(\frac{\partial^2 u(x,y)}{\partial x^2}\right)_N$ be the CWA of $\left(\frac{\partial^2 u(x,y)}{\partial x^2}\right)$ and assume that the mixed derivative of $\left(\frac{\partial^2 u(x,y)}{\partial x^2}\right)$ is bounded by a constant S_2.i.e. $\left|\frac{\partial^3 u(x,y)}{\partial x^2 \partial y}\right| < S_2$, then we have the following upper bound of error:*

$$\left\|\frac{\partial^2 u(x,y)}{\partial x^2} - \left(\frac{\partial^2 u(x,y)}{\partial x^2}\right)_N\right\|_{L^2}^2 < \frac{S_2^2}{2}(F[1,N])^2,$$

where, $F[1,N]$ is polygamma function.

Proof Proof is similar as *theorem* (4.5.3).

4.6 Error Bound

Let $e_N(x,y) = u(x,y) - u_N(x,y)$ be the error function of Legendre and Chebyshev wavelets approximation solution $u_N(x,y)$ to $u(x,y)$, where $u(x,y)$ is the exact solution of $Eq.(4.1)$.

Substituting the approximate solution into $Eq.(4.1)$, we get

$Type-I \;\; error$:

$$(u_y)_N + R_N(x,y) = u_N(x,y) + f(x,y) + \int_0^x \int_0^y \frac{(u_{tt})_N(s,t)}{(x-s)^\alpha} dtds, \tag{4.38}$$

with $(u(x,0))_N = (u_0(x))_N$,

where, $R_N(x,y)$ is the perturbation function that depends on $u_N(x,y)$, $((u_{tt})_N(x,y))$, $(u_y(x,y))_N$ and $(u(x,0))_N$.

It can be evaluated as

$$R_N(x,y) = f(x,y) + u_N(x,y) + \int_0^x \int_0^y \frac{(u_{tt})_N(s,t)}{(x-s)^\alpha} dtds - (u_y)_N,$$

so

$$(e_y)_N - R_N(x,y) = e_N(x,y) + \int_0^x \int_0^y \frac{(e_{tt})_N(s,t)}{(x-s)^\alpha} dtds,$$

or,

$$(e_y)_N = R_N(x,y) + e_N(x,y) + \int_0^x \int_0^y \frac{(e_{tt})_N(s,t)}{(x-s)^\alpha} dtds, \tag{4.39}$$

with the initial condition $(e(x,0))_N = (e_0(x))_N$.

To compute an error approximation of $e_N(x,y)$ in $Eq.(4.39)$, the proposed method in this chapter can be applied.

By grouping lemma $(4.5.2 - 4.5.3)$ and $(4.5.5 - 4.5.6)$, we will prove that the error term $e_N \to 0$ as $N \to \infty$.

Since, from $Eq.(4.1)$ we have

$$u(x,y) = u_y(x,y) - f(x,y) - \int_0^x \int_0^y \frac{u_{tt}(s,t)}{(x-s)^\alpha} dtds, \qquad 0 \le s \le x,\ 0 \le t \le y, \quad (4.40)$$

and approximate solution of $u(x,y)$ as :

$$u_N(x,y) = (u_y)_N(x,y) - f_N(x,y) - \int_0^x \int_0^y \frac{(u_{tt})_N(s,t)}{(x-s)^\alpha} dtds. \quad (4.41)$$

Subtracting $Eq.(4.41)$ from equation $Eq.(4.40)$, we get

$$(u - u_N) = (u_y - (u_y)_N) - (f - f_N) - \int_0^x \int_0^y \frac{(u_{tt} - (u_{tt})_N)}{(x-s)^\alpha} dtds,$$

taking $L^2 - norm$ both side, we get

$$\| u - u_N \| \le \| u_y - (u_y)_N \| + \| f - f_N \| + \int_0^x \int_0^y \| \frac{(u_{tt} - (u_{tt})_N)}{(x-s)^\alpha} \| dsdt,$$

or,

$$\| u - u_N \| \le \| u_y - (u_y)_N \| + \| f - f_N \| + \| u_{xx} - (u_{xx})_N \| \int_0^x \int_0^y \frac{1}{(x-s)^\alpha} dsdt,$$

or,

$$\| u - u_N \| \le \| u_y - (u_y)_N \| + \| f - f_N \| + \| u_{xx} - (u_{xx})_N \| \frac{x^{1-\alpha}}{1-\alpha}.$$

This is error bound for $Type - I$ *error.*

Now, see following theorem for $Type - II$ and $Type - III$ *error.*

Theorem 4.6.1 *Let $u(x,y)$ be the exact solution and $u_N(x,y) = E^T\Phi(x,y)$ be the Legendre and Chebyshev wavelets approximation solution of Eq.(4.1) under the following mild conditions on integral:*

1.Function of kernal is integrable on Ω

2.Non-linear term $Bu(x,y)$ satisfies the Lipschitz condition in $L^2(\Omega)$ such that

$$\|Bu(x,y) - Bu_N(x,y)\|_{L^2} \leq \vartheta \|u(x,y) - u_N(x,y)\|_{L^2}, \ \forall (x,y) \in \Omega,$$

where $\vartheta > 0$ is Lipschitz constant. Then the error bound of $Type-II$ and $Type-III$ as follows:

$$\|u - u_N\|_{L^2} \leq \frac{1-\alpha}{1-\alpha-x^{1-\alpha}} \left(\|u_y - (u_y)_N\|_{L^2} + \|f - f_N\|_{L^2} \right).$$

Proof Since Legendre and Chebyshev wavelets approximation solution of $Eq.(4.1)$ as follows:

$$u_N(x,y) = (u_y)_N(x,y) - f_N(x,y) - \int_0^x \int_0^y \frac{Bu_N(s,t)}{(x-s)^\alpha} dtds, \tag{4.42}$$

then subtracting $Eq.(4.42)$ from equation $Eq.(4.1)$, we get

$$(u - u_N) = (u_y - (u_y)_N) - (f - f_N) - \int_0^x \int_0^y \frac{Bu - Bu_N}{(x-s)^\alpha} dtds,$$

taking $L^2 - norm$ both side,we get

$$\| u - u_N \| \leq \| u_y - (u_y)_N \| + \| f - f_N \| + \int_0^x \int_0^y \| \frac{Bu - Bu_N}{(x-s)^\alpha} \| dsdt,$$

or

$$\|u - u_N\| \leq \|u_y - (u_y)_N\| + \|f - f_N\| + \vartheta \|u - (u_N\| \int_0^x \int_0^y \frac{1}{(x-s)^\alpha} dsdt,$$

or,

$$\|u - u_N\| \leq \|u_y - (u_y)_N\| + \|f - f_N\| + \vartheta \|u_-(u_N\| \frac{x^{1-\alpha}}{1-\alpha},$$

or,

$$\|u - u_N\| \leq \frac{1-\alpha}{1-\alpha-x^{1-\alpha}} \left(\|u_y - (u_y)_N\| + \|f - f_N\| \right).$$

4.7 Error Estimation

Let $e_N(x,y) = u(x,y) - u_N(x,y)$ be the error function of approximate solution $u_N(x,y)$ to $u(x,y)$, where $u(x,y)$ is the exact solution of $Eq.(4.1)$.

Substituting the approximate solution into $Eq.(4.1)$, we get

$$(u_y)_N + R_N(x,y) = u_N(x,y) + f(x,y) + \int_0^x \int_0^y \frac{(Bu_N(s,t)}{(x-s)^\alpha} dtds, \tag{4.43}$$

with $(u(x,0))_N = (u_0(x))_N$,

where, $R_N(x,y)$ is the perturbation function that depends on $u_N(x,y)$, $(Bu_N(x,y))$, $(u_y(x,y))_N$ and $(u(x,0))_N$.

It can be evaluated as

$$R_N(x,y) = f(x,y) + u_N(x,y) + \int_0^x \int_0^y \frac{Bu_N(s,t)}{(x-s)^\alpha} dtds - (u_y)_N,$$

so

$$(e_y)_N - R_N(x,y) = e_N(x,y) + \int_0^x \int_0^y \frac{Be_N(s,t)}{(x-s)^\alpha} dtds,$$

or,

$$(e_y)_N = R_N(x,y) + e_N(x,y) + \int_0^x \int_0^y \frac{Be_N(s,t)}{(x-s)^\alpha} dtds, \tag{4.44}$$

with the initial condition $(e(x,0))_N = (e_0(x))_N$.

To compute an error approximation of $e_N(x,y)$ in $Eq.(4.44)$, the proposed method in this chapter can be applied.

By grouping theorems and lemmas, we can see that the error term $e_N \to 0$ as $N \to \infty$.

4.8 Numerical examples

In this section, we took five literature examples (see [177]). These examples are given to demonstrate the efficiency and accuracy of our proposed method using Legendre wavelet approximation (LWA) as well as Chebyshev wavelet approximation (CWA) with the basis function at $k = k' = 1, M = M' = 3$ (see figures 4.1−4.4) and for application of piecewise basis decomposition ($k = k' = 1$ to $k = k' = 3$) in example 4.5 and figures $4.5 - 4.9$. Also, we are given absolute error tables 4.2 and 4.4 for examples $4.1 - 4.1$, $l_2 - error$ table 4.3, $4.5 - 4.6$ and $l_\infty - error$ tables 4.3, $4.5 - 4.6$ for example $4.1 - 4.4$.

Example 4.1 Consider the following partial integro-differential equation of $Type-I$ with $\alpha = 1/4$, $k = k' = 1$ and $M = M' = 3$ (see [177]):

$$u_y = u(x,y) + f(x,y) + \int_0^x \int_0^y \frac{u_{tt}(s,t)}{(x-s)^\alpha} dtds,$$

subject to initial condition $u(x,0) = 0$, and $f(x,y) = 2xy - xy^2 - \frac{32}{21}x^{7/4}y$.

For these conditions there is known analytical solution $u(x,y) = xy^2$ (see Fig 1(a) and Fig 1(b)).

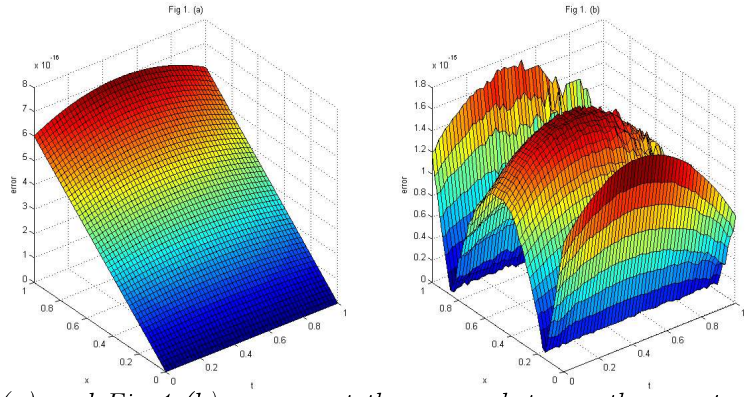

Figure 4.1: Fig 1.(a) and Fig 1.(b), represent the errors between the exact solution of example 4.1 and its numerical solution to utilising the LWA and CWA respectively for $k = k' = 1, M = M' = 3$.

Example 4.2 Consider the following partial integro-differential equation of $Type-I$ with $\alpha = 1/4$, $k = k' = 1$ and $M = M' = 3$ (see [177]):

$$u_y = u(x,y) + f(x,y) + \int_0^x \int_0^y \frac{u_{tt}(s,t)}{(x-s)^\alpha} dtds$$

subject to initial condition $u(x,0) = x^2$, and

$$f(x,y) = 2y - x^2 - y^2 - \frac{2}{15}(x^{5/2}y + 5x^{1/2}y^3)$$

For these conditions there is known simple known analytical solution $u(x,y) = x^2 + y^2$ (see Fig 2(a) and Fig 2(b)).

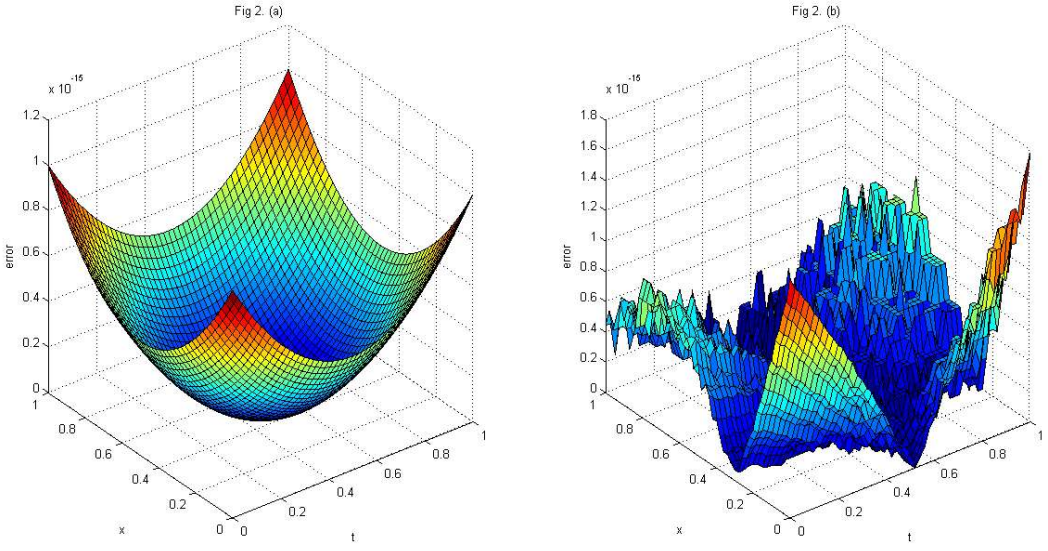

Figure 4.2: Fig 2.(a) and Fig 2.(b), represent the errors between the exact solution of example 4.2 and its numerical solution to utilising the LWA and CWA respectively for $k = k' = 1, M = M' = 3$.

Example 4.3 Consider the following partial integro-differential equation of $Type-II$ with $\alpha = 1/2,\ p = 2,\ k = k' = 1$ and $M = M' = 3$ (see [177])):

$$u_y = u(x,y) + f(x,y) + \int_0^x \int_0^y \frac{[u(\zeta,\eta)]^p}{(x-\zeta)^\alpha} d\eta d\zeta$$

subject to initial condition $u(x,0) = x^2$, and

$$f(x,y) = 2y - x^2 - y^2 - \frac{2}{315} x^{1/2} y(125x^4 + 112x^3y^2 + 63x^4)$$

For these conditions there is known simple known analytical solution $u(x,y) = x^2 + y^2$. (see Fig 3(a) and Fig 3(b)).

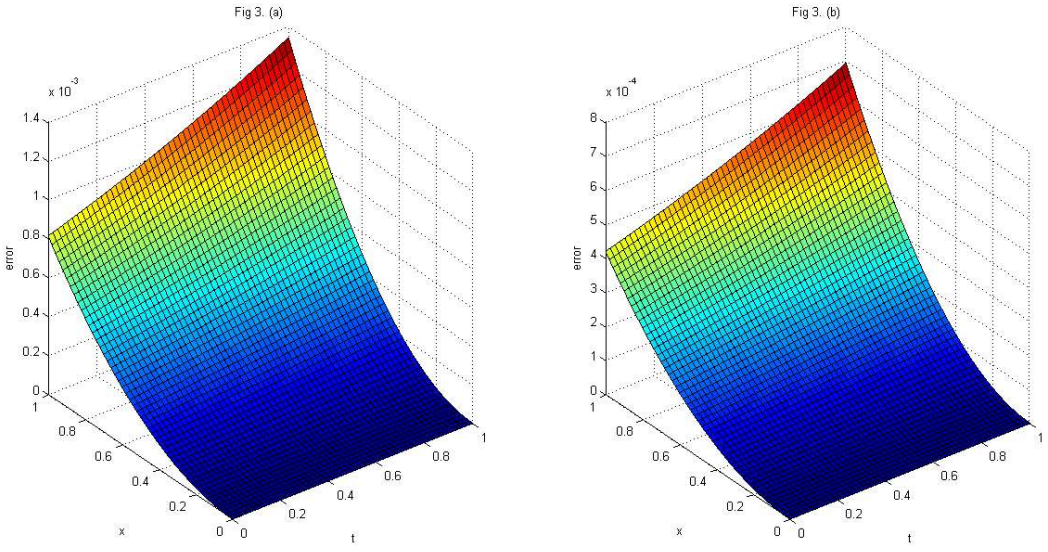

Figure 4.3: Fig 3.(a) and Fig 3.(b), represent the errors between the exact solution of example 4.3 and its numerical solution to utilising the LWA and CWA respectively for $k = k' = 1, M = M^{'} = 3$.

Example 4.4 Consider the following partial integro-differential equation of $Type-III$ with $\alpha = 1/4, i = 1, j = 0, p = 2, k = k' = 1$ and $M = M' = 3$ (see [177]):

$$u_y = u(x,y) + f(x,y) + \int_0^x \int_0^y \frac{[\gamma_{i,j} u(\zeta,\eta)]^p}{(x-\zeta)^\alpha} d\eta d\zeta$$

subject to initial condition $u(x,0) = 0$, and

$$f(x,y) = x^2 cosy - x^2 siny - \frac{32}{15} x^{5/2}(y - siny\ cosy)$$

For these conditions there is known simple known analytical solution $u(x,y) = x^2 siny$. (see Fig 4(a) and Fig 4(b)).

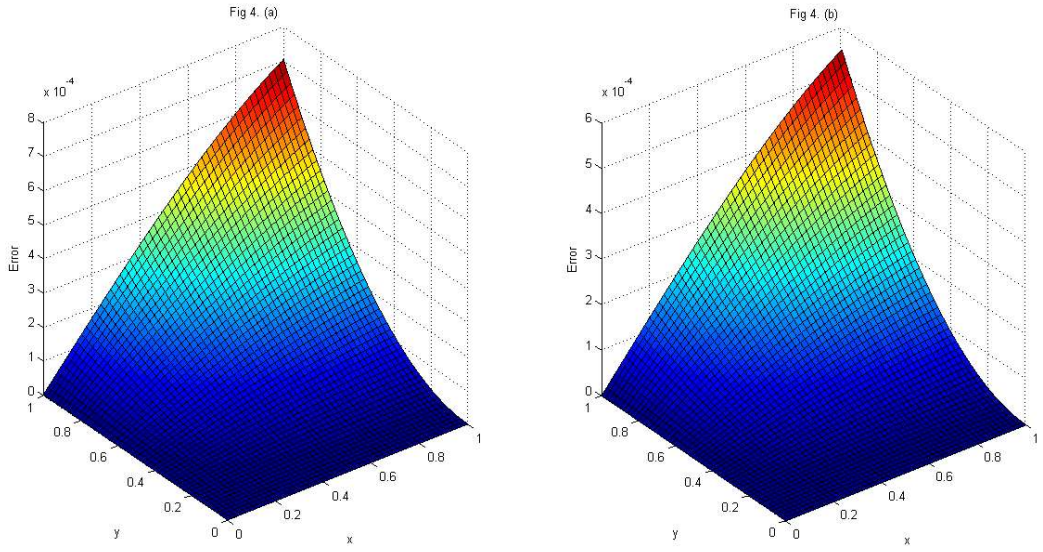

Figure 4.4: Fig 4.(a) and Fig 4.(b), represent the errors between the exact solution of example 4.4 and its numerical solution to utilising the LWA and CWA respectively for $k = k' = 1, M = M' = 3$.

Example 4.5 Consider the following partial integro-differential equation of $Type-I$ with $\alpha = 1/4$,

$$u_y = u(x,y) + f(x,y) + \int_0^x \int_0^y \frac{u_{tt}(s,t)}{(x-s)^\alpha} dtds$$

subject to initial condition $u(x,0) = x^2$, and

$$f(x,y) = -2e^{-y}x^2 - \frac{128}{231}e^{-y}(-1+e^{-y})x^{\frac{11}{4}}$$

For these conditions there is known simple known analytical solution $u(x,y) = x^2e^{-y}$ and basis function at $M = M' = 3$.

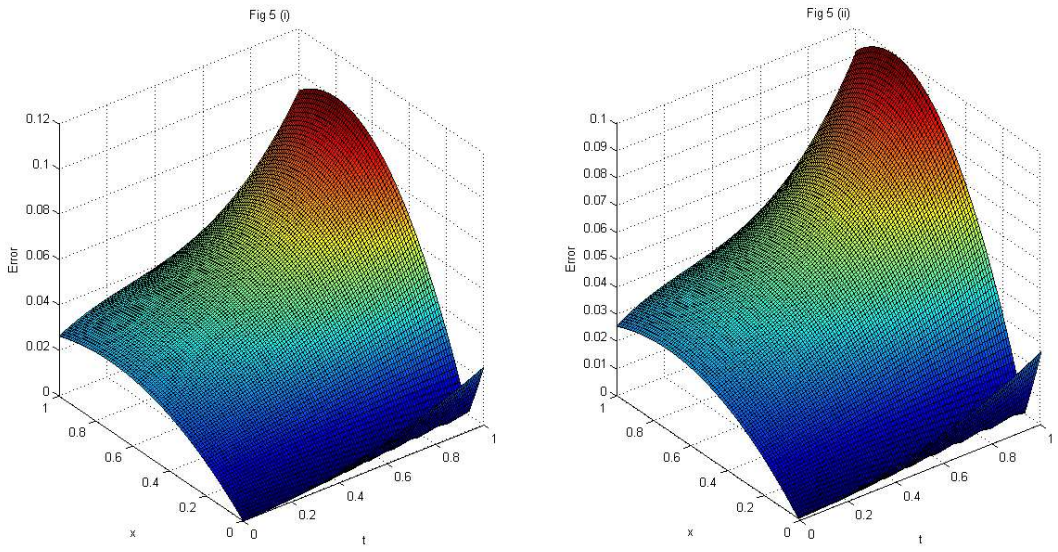

Figure 4.5: Fig 5(i), represent the errors between the exact solution of example 4.5 and its numerical solution to utilising the LWA for $k = k' = 1, n = n' = 1$) and Fig 5(ii), represent the errors between the exact solution of example 4.5 and its numerical solution to utilising the CWA for $k = k' = 1, n = n' = 1$.

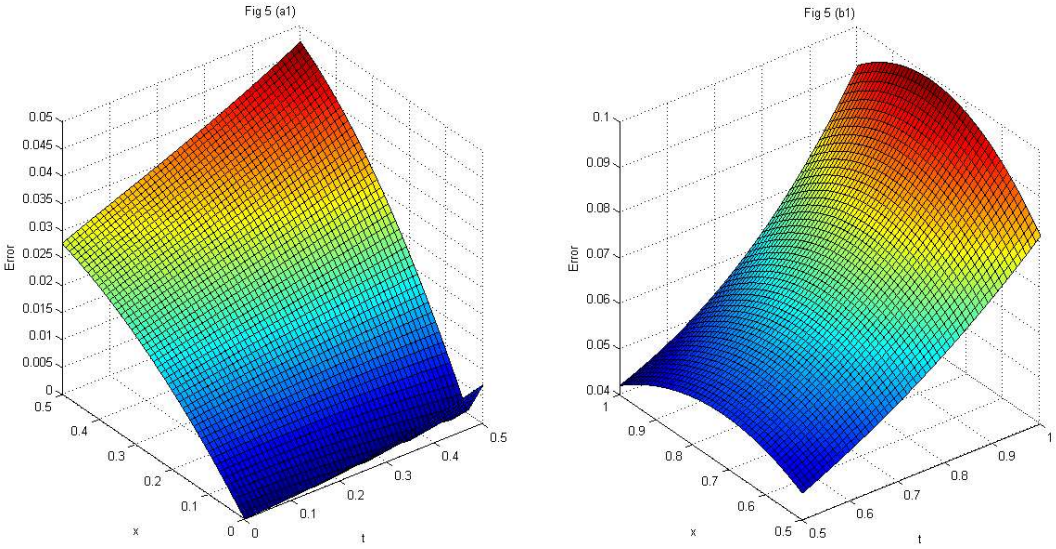

Figure 4.6: *Fig 5* (a_1)*, represent the errors between the exact solution of example 4.5 and its numerical solution to utilising the LWA for* $k = k' = 2, n = n' = 1$ *and Fig 5* (b_1)*, represent the errors between the exact solution of example 4.5 and its numerical solution to utilising the LWA for* $k = k' = 2, n = n' = 2$*.*

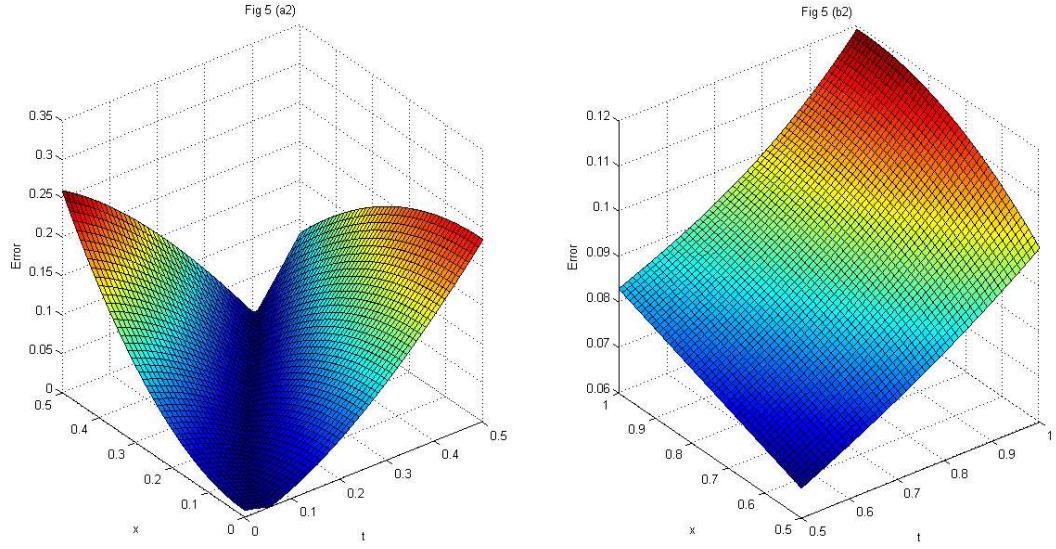

Figure 4.7: *Fig 5* (a_2)*, represent the errors between the exact solution of example 4.5 and its numerical solution to utilising the CWA for* $k = k' = 2, n = n' = 1$ *and Fig 5* (b_2)*, represent the errors between the exact solution of example 4.5 and its numerical solution to utilising the CWA for* $k = k' = 2, n = n' = 2$*.*

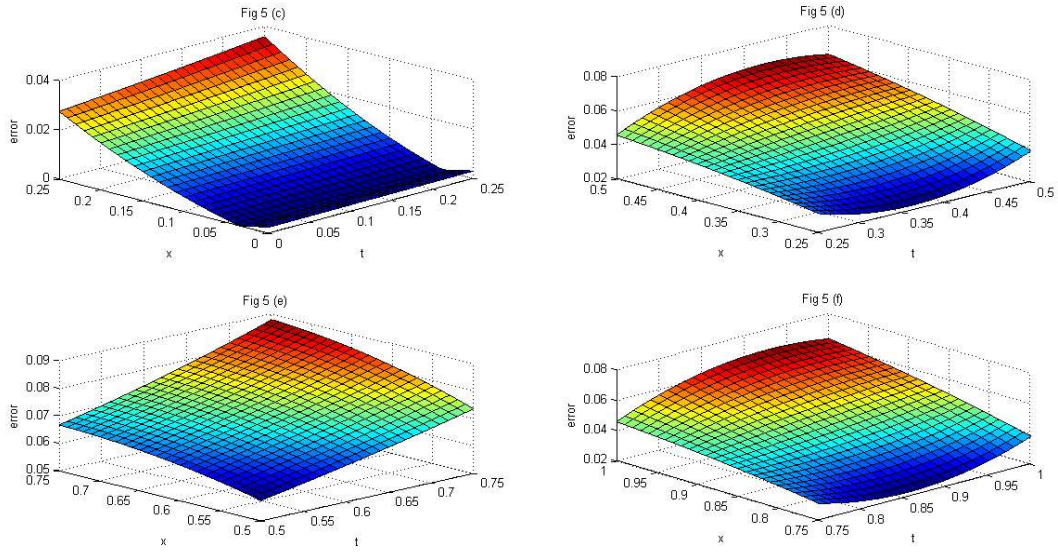

Figure 4.8: *Fig 5(c), represent the errors between the exact solution of example 4.5 and its numerical solution to utilising the LWA for* $k = k' = 3, n = n' = 1$*, Fig 5(d), represent the errors between the exact solution of example 4.5 and its numerical solution to utilising the LWA for* $k = k' = 3, n = n' = 2$*, Fig 5 (e), represent the errors between the exact solution of example 4.5 and its numerical solution to utilising the LWA for* $k = k' = 3, n = n' = 3$ *and Fig 5 (f), represent the errors between the exact solution of example 4.5 and its numerical solution to utilising the LWA for* $k = k' = 3, n = n' = 4$.

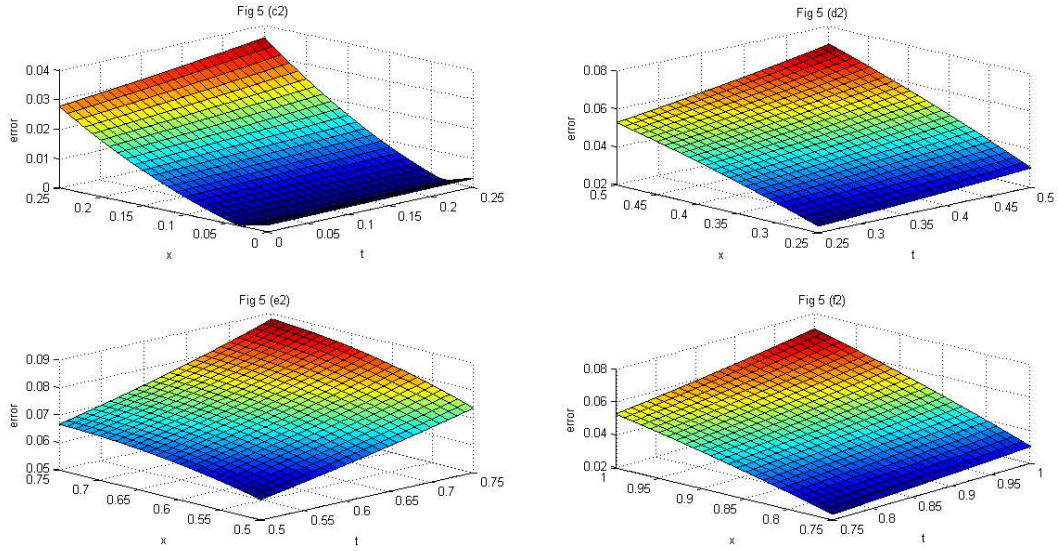

Figure 4.9: Fig 5 (c2), represent the errors between the exact solution of example 4.5 and its numerical solution to utilising the CWA for $k = k' = 3, n = n' = 1$, Fig 5 (d2), represent the errors between the exact solution of example 4.5 and its numerical solution to utilising the CWA for $k = k' = 3, n = n' = 2$, Fig 5 (e2), represent the errors between the exact solution of example 4.5 and its numerical solution to utilising the CWA for $k = k' = 3, n = n' = 3$ and Fig 5 (f2), represent the errors between the exact solution of example 4.5 and its numerical solution to utilising the CWA for $k = k' = 3, n = n' = 4$.

Example 4.6 Consider the following partial integro-differential equation of $Type-I$ with $\alpha = 1/4$:

$$u_y = u(x,y) + f(x,y) + \int_0^x \int_0^y \frac{u_{tt}(s,t)}{(x-s)^\alpha} dtds,$$

subject to initial condition $u(x,0) = 0$, and

$$f(x,y) = x^{m+\alpha}\left(y - y^2 - 2yx^{3/4}\frac{\Gamma(\frac{3}{4})\Gamma(1+m+\alpha)}{\Gamma(\frac{7}{4}+m+\alpha)}\right).$$

For these conditions there is known analytical solution $u(x,y) = x^{m+\alpha}y^2$, here m is the number of basis function and $0 < \alpha < 1$.

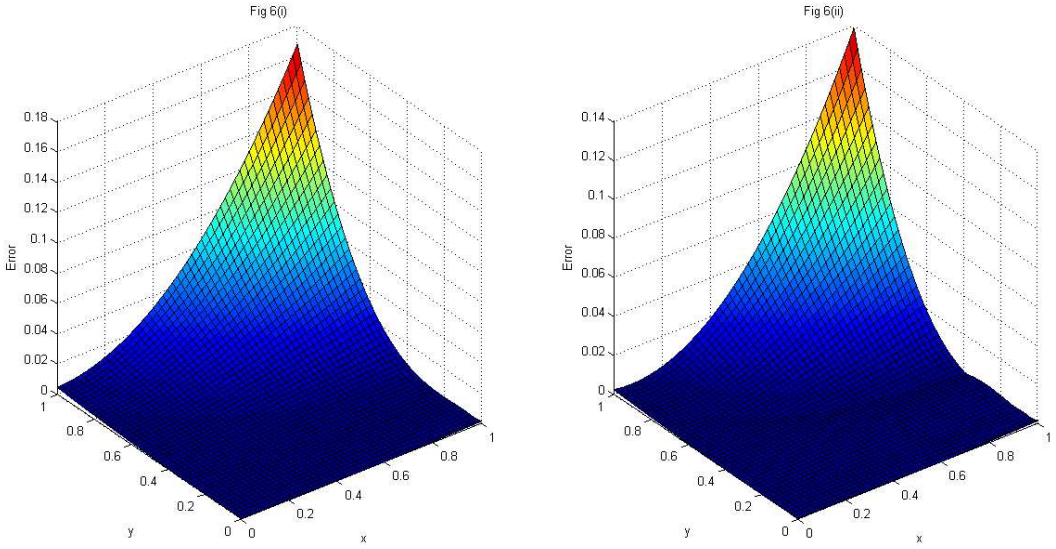

Figure 4.10: Fig 6(i), represent the errors between the exact solution of example 4.6 *and its numerical solution to utilising the LWA for* $k = k' = 1$ *(so,* $n = n' = 1$*) and Fig 6(ii), represent the errors between the exact solution of example* 4.6 *and its numerical solution to utilising the CWA for* $k = k' = 1$*.*

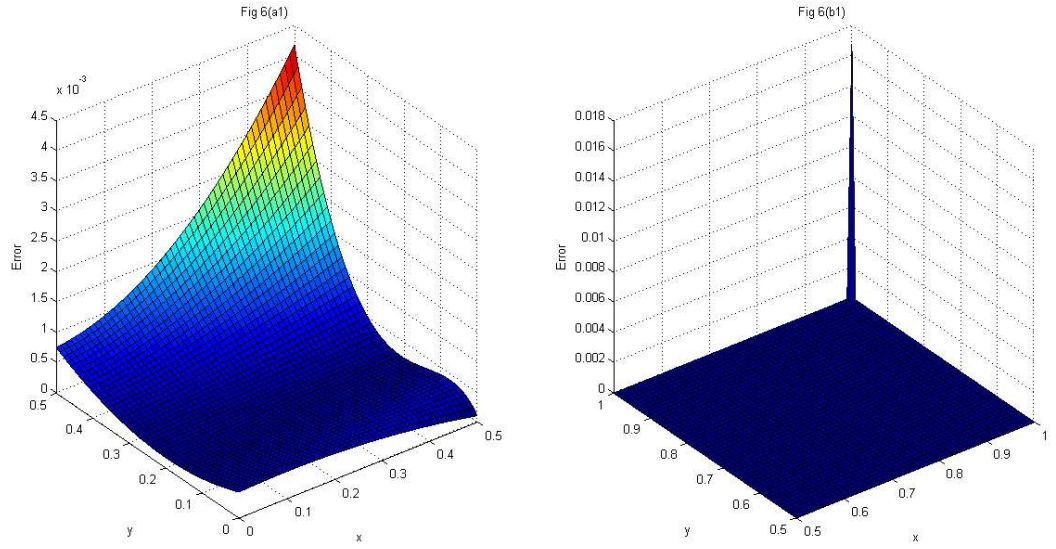

Figure 4.11: Fig 6 (a_1)*, represent the errors between the exact solution of example* 4.6 *and its numerical solution to utilising the LWA for* $k = k' = 2, n = n' = 1$ *and Fig 6* (b_1)*, represent the errors between the exact solution of example* 4.6 *and its numerical solution to utilising the LWA for* $k = k' = 2, n = n' = 2$*.*

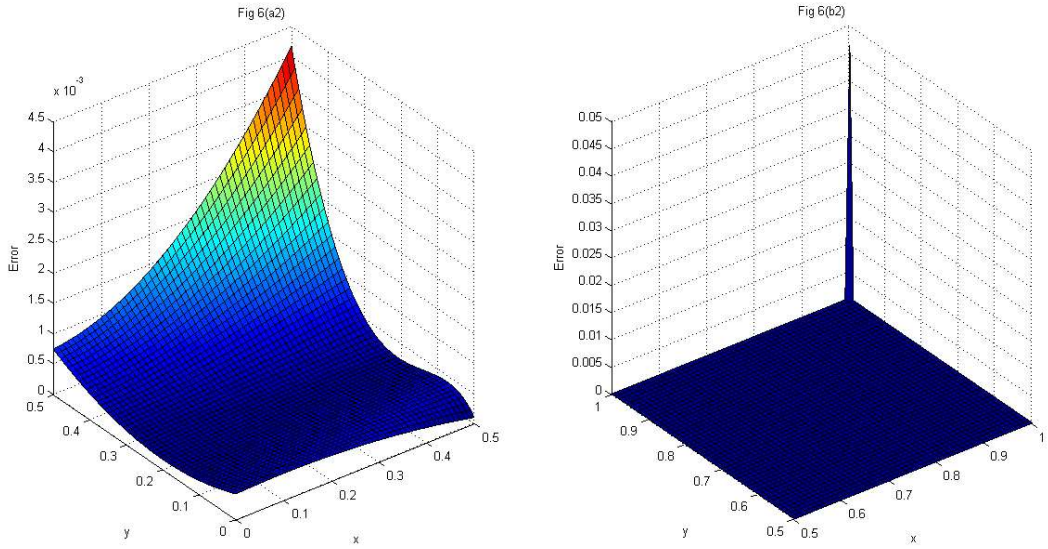

Figure 4.12: *Fig 6* (a_2)*, represent the errors between the exact solution of example* 4.6 *and its numerical solution to utilising the CWA for* $k = k' = 2, n = n' = 1$ *and Fig 6* (b_2)*, represent the errors between the exact solution of example* 4.6 *and its numerical solution to utilising the CWA for* $k = k' = 2, n = n' = 2$.

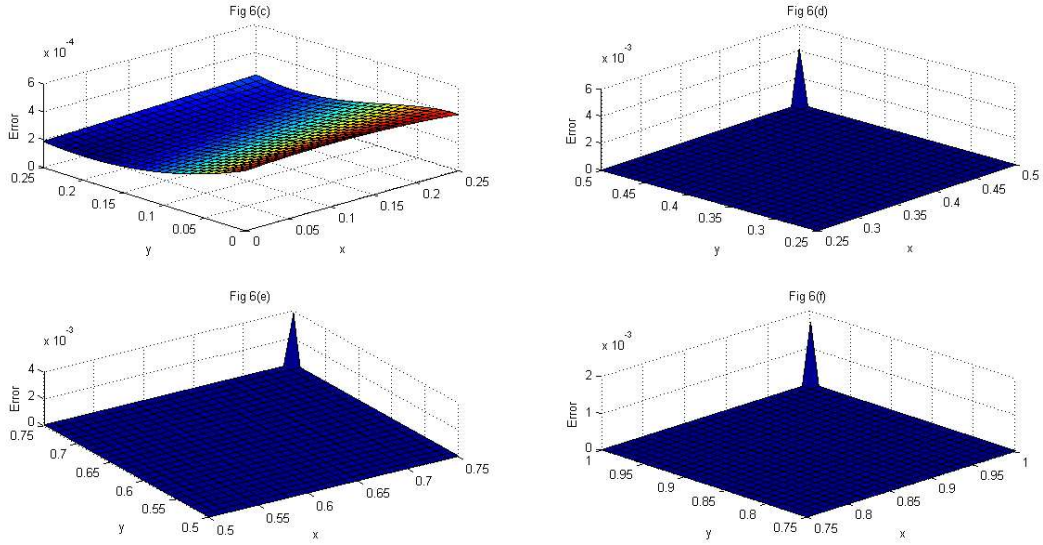

Figure 4.13: *Fig 6(c), represent the errors between the exact solution of example* 4.6 *and its numerical solution to utilising the LWA for* $k = k' = 3, n = n' = 1$*, Fig 6(d), represent the errors between the exact solution of example 4.6 and its numerical solution to utilising the LWA for* $k = k' = 3, n = n' = 2$*, Fig 6 (e), represent the errors between the exact solution of example 4.6 and its numerical solution to utilising the LWA for* $k = k' = 3, n = n' = 3$ *and Fig 6 (f), represent the errors between the exact solution of example 4.6 and its numerical solution to utilising the LWA for* $k = k' = 3, n = n' = 4$.

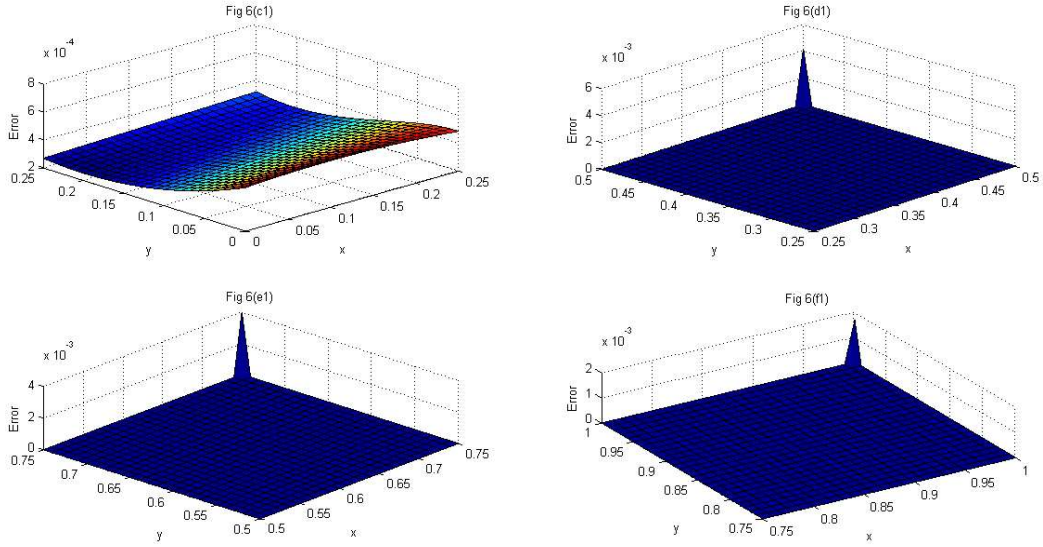

Figure 4.14: Fig 6 (c1), represent the errors between the exact solution of example 4.6 *and its numerical solution to utilising the CWA for* $k = k' = 3, n = n' = 1$*, Fig 6 (d1), represent the errors between the exact solution of example 4.6 and its numerical solution to utilising the CWA for* $k = k' = 3, n = n' = 2$*, Fig 6 (e1), represent the errors between the exact solution of example 4.6 and its numerical solution to utilising the CWA for* $k = k' = 3, n = n' = 3$ *and Fig 6 (f1), represent the errors between the exact solution of example 4.6 and its numerical solution to utilising the CWA for* $k = k' = 3, n = n' = 4$.

Table 4.2: Absolute error for $k = k' = 1$ and $M = M' = 3$

(x,y)	**Example 4.1 for LWA**	**Example 4.1 for CWA**	**Example 4.2 for LWA**	**Example 4.2 for CWA**
$(0.1, 0.1)$	6.4e-16	7.6e-16	6.3e-16	4.1e-16
$(0.2, 0.2)$	3.6e-16	2.2e-16	1.3e-15	4.4e-16
$(0.3, 0.3)$	1.6e-16	2.0e-17	2.1e-15	1.1e-15
$(0.4, 0.4)$	4.0e-17	1.1e-16	2.8e-15	1.6e-15
$(0.5, 0.5)$	0.0e-16	1.1e-16	3.5e-15	1.7e-15
$(0.6, 0.6)$	4.0e-17	0.0e-16	4.2e-15	1.5e-15
$(0.7, 0.7)$	1.6e-16	3.3e-16	4.9e-15	9.9e-16
$(0.8, 0.8)$	0.0e-16	4.4e-16	5.3e-15	4.4e-16
$(0.9, 0.9)$	0.0e-16	4.4e-16	5.7e-15	4.4e-16
$(1.0, 1.0)$	0.0e-16	0.0e-16	6.0e-15	7.7e-16

Table 4.3: l_2 and l_∞ error for $k = k' = 1$ and $M = M' = 3$

Norm *Space*	**Example 4.1 for LWA**	**Example 4.1 for CWA**	**Example 4.2 for LWA**	**Example 4.2 for CWA**
l_2	7.7e-16	1.1e-15	1.3e-14	3.4e-15
l_∞	6.4e-14	7.6e-16	6.0e-15	1.7e-15

Table 4.4: Absolute error for $k = k' = 1$ and $M = M' = 3$

(x,y)	**Example 4.3 for LWA**	**Example 4.3 for CWA**	**Example 4.4 for LWA**	**Example 4.4 for CWA**
$(0.1, 0.1)$	4.2e-5	4.2e-5	0.0e-6	0.0e-6
$(0.2, 0.2)$	1.8e-4	1.7e-5	3.3e-6	2.6e-6
$(0.3, 0.3)$	4.4e-4	4.1e-5	1.5e-5	1.3e-5
$(0.4, 0.4)$	8.3e-4	7.8e-4	3.9e-5	3.1e-5
$(0.5, 0.5)$	1.4e-4	1.3e-4	8.1e-5	6.3e-5
$(0.6, 0.6)$	2.1e-4	1.9e-4	1.4e-4	1.2e-4
$(0.7, 0.7)$	2.9e-4	2.7e-4	2.3e-4	1.8e-4
$(0.8, 0.8)$	4.1e-4	3.8e-4	3.4e-4	2.6e-4
$(0.9, 0.9)$	5.4e-4	5.1e-4	4.8e-4	3.8e-4
$(1.0, 1.0)$	7.4e-4	6.9e-4	7.0e-4	5.4e-4

Table 4.5: l_2 error for $k = k' = 1$ and $M = M' = 3$

Iteration number	**Example 4.3 for LWA**	**Example 4.3 for CWA**	**Example 4.4 for LWA**	**Example 4.4 for CWA**
1	3.2e-2	4.2e-2	0.2e-2	0.3e-2
2	2.8e-3	1.7e-3	3.3e-3	2.6e-3
2	5.4e-4	4.1e-4	1.5e-4	1.3e-4
4	8.7e-4	7.8e-4	3.9e-4	8.1e-5

Table 4.6: l_∞ error for $k = k' = 1$ and $M = M' = 3$

Iteration number	**Example 4.3 for LWA**	**Example 4.3 for CWA**	**Example 4.4 for LWA**	**Example 4.4 for CWA**
1	4.2e-2	4.2e-3	0.1e-3	0.3e-3
2	2.8e-3	1.7e-3	3.3e-3	2.6e-3
2	4.4e-4	4.1e-4	1.5e-4	4.3e-4
4	9.3e-4	7.8e-4	7.9e-5	3.1e-4

4.9 Conclusion

We studied comparative study of two different approximation scheme based on two dimensional Legendre and Chebyshev wavelets approximation respectively for linear and nonlinear partial integro-differential equations(PIDEs) with weak singularity. Implementation of two dimensional wavelets operational matrices to find the numerical solution of weakly singular PIDEs is still going on and previous results of numerical methods for PIDEs are encouraging (see [177]). In this chapter, we analysed the solution of *Eq.*(4.1) based on two-dimensional Legendre and Chebyshev wavelets operational matrices and we derived three different variant of the proposed problem. The $type - I$ is linear PIDE, $type - II$ is nonlinear PIDEs without derivative term in the integration of *Eq.*(4.1) and the last $type - III$ is nonlinear PIDE with derivative term in the integration of *Eq.*(4.1). A smoothness condition is introduced to find the numerical schemes for linear and nonlinear PIDE. We investigated convergence, error analysis, error bound and error estimation (see *Eq.*(4.44)) via Legendre and Chebyshev wavelets approximation for linear and nonlinear PIDE respectively. The validity and applicability of the schemes are illustrated by the several examples. Numerical results of linear PIDE via Examples $4.1 - 4.2$, presented in Tables $4.2 - 4.3$ and numerical results of nonlinear PIDE

via Examples $4.3 - 4.4$, presented in Tables $4.4 - 4.5$ respectively. Also, we have discussed the application of piecewise approximation based on operational matrices (see construction of piecewise wavelet operational matrices in Appendix section 6.2) of Legendre and Chebyshev wavelets via Examples $(4.5 - 4.6)$ and one can detect that the errors are slightly larger for $k = k' = 1, M = M' = 3$, see Figures 4.5 and 4.10. So, for reducing errors, we divided $2D$ interval at $k = k' = 2, M = M' = 3$ and $k = k' = 3, M = M' = 3$, see Figures $4.6 - 4.9$ and $4.10 - 4.14$. Hence, we may conclude through the Figures $4.5 - 4.9$, that piecewise approximation is getting better approximation. Finally, It is concluded that both the wavelets approximation scheme perform well, simple, effective and provides accurate numerical results as possible as. It is also observed that the performance of the method depends on the nature of the problem and the discussed methods successfully validate the numerical results.

****